



## Inducing local T cell apoptosis with anti-Fas-functionalized polymeric coatings fabricated via surface-initiated photopolymerizations

Patrick S. Hume<sup>a</sup>, Kristi S. Anseth<sup>a,b,\*</sup>

<sup>a</sup>Department of Chemical and Biological Engineering, University of Colorado, 424 UCB, Boulder, CO 80309, USA

<sup>b</sup>The Howard Hughes Medical Institute, University of Colorado, Boulder, CO 80309, USA

### ARTICLE INFO

#### Article history:

Received 24 November 2009

Accepted 9 January 2010

Available online 5 February 2010

#### Keywords:

Apoptosis

Immunomodulation

Lymphocyte

Photopolymerization

Surface modification

### ABSTRACT

Cell encapsulation has long been investigated as a means to achieve transplant immunoprotection as it creates a physical barrier between allograft tissue and host immune cells. Encapsulation with passive barrier materials alone, however, is generally insufficient to protect donor tissue from rejection, because small cytotoxic molecules produced by activated T cells can diffuse readily into the capsule and mediate allograft death. As a means to provide bioactive protection for polymeric encapsulation devices, we investigated a functionalized polymeric coating that mimics a natural T cell regulation pathway. T cells are regulated *in vivo* via Fas, a well-known 'death receptor,' whereby effector cells express Fas ligand and elicit T cell apoptosis upon binding the Fas receptor on a T cell surface. Anti-Fas antibodies are capable of replicating this effect and induce T cell apoptosis in solution. Here, an iniferter-based living radical polymerization was utilized to fabricate surface-anchored polymer chains containing poly(ethylene glycol) with covalently incorporated pendant anti-Fas antibody. Using this reaction mechanism, we demonstrate fabrication conditions that yield surface densities in excess of 1.5 ng/cm<sup>2</sup> of incorporated therapeutic, as detected by ELISA. Additionally, we show that coatings containing anti-Fas antibody induced significant T cell apoptosis, 21 ± 2% of cells, after 24 h. Finally, the incorporation of a T cell adhesion ligand, intracellular adhesion molecule-1, along with anti-Fas antibody, yielded even higher levels of apoptosis, 34 ± 1% of T cells, compared to either signal alone.

Published by Elsevier Ltd.

### 1. Introduction

Cell transplantation has the potential to cure numerous diseases of the endocrine, cardiovascular, and central nervous systems [1–3]. However, clinical prevalence of allogeneic cell transplantation is limited due, in part, to the side effects of immunosuppressants administered systemically for suppressing host immune rejection [4]. Encapsulating donor cells within immunoisolation barrier materials has been widely explored as a means to decrease the necessity of systemic immunosuppression, because the barrier materials can block direct contact between the transplanted grafts and the host immune cells [4]. For example, the encapsulation of pancreatic  $\beta$ -cells for the treatment of type I diabetes mellitus has been extensively studied over the last 30 years [5,6]. An important criterion of designing materials for immunoisolation is that the capsule should block immune cell contact, but must not restrict the

diffusion of small molecules such as nutrients, glucose, and insulin, as they are necessary for maintaining  $\beta$ -cell survival and transplant function. While maintaining permeability of the capsule is critical, it has been shown that small cytotoxic molecules produced by activated, autoreactive T lymphocytes are capable of infiltrating the capsule and inducing donor cell apoptosis [7–9]. These cytotoxic molecules include reactive oxygen species (ROS), interleukin 1 $\beta$  (IL-1 $\beta$ ), and tumor necrosis factor alpha (TNF- $\alpha$ ), etc. While the material properties of the encapsulation systems are improving [10], systemic immunosuppression remains necessary for the long-term (>1 yr) survival of encapsulated  $\beta$ -cells [11,12].

Recently, efforts have been made to fabricate bioactive encapsulation barriers capable of regulating the local immune environment. For example, a polymerizable superoxide dismutase mimetic has been described which catalyzes the dismutation of superoxide into hydrogen and oxygen when co-photopolymerized with poly(ethylene glycol)-diacrylate (PEGDA) [13]. Likewise, methods to conjugate antibodies or peptides which sequester TNF- $\alpha$  within encapsulation materials have been developed to slow cytokine diffusion and improve encapsulated cell viability [14,15]. Unlike these approaches, which regulate the capsule's internal cytokine

\* Corresponding author. Department of Chemical and Biological Engineering, University of Colorado, 424 UCB, Boulder, CO 80309, USA.

E-mail address: [Kristi.Anseth@Colorado.edu](mailto:Kristi.Anseth@Colorado.edu) (K.S. Anseth).

environment, we report an alternate strategy to functionalize the surface of polymeric encapsulation materials, such as PEGDA hydrogels, to modulate the immune reactions by inducing local T lymphocyte apoptosis.

Previously, research has investigated strategies to induce T lymphocyte apoptosis utilizing Fas signaling [16]. Fas, a cell surface receptor in the TNF- $\alpha$  superfamily, induces apoptosis upon Fas ligand (FasL) binding. The Fas pathway plays two important roles in normal lymphocyte regulation. First, autoreactive T cells undergo negative selection via clonal deletion mediated by Fas/FasL signaling [17]. Second, T cells strongly upregulate Fas expression upon activation, and FasL-expressing cytotoxic lymphocytes induce T cell apoptosis to clear a completed immune response [18]. To initiate the signal transduction cascade resulting in cell apoptosis, pre-associated Fas receptors on the cell membrane must bind multiple FasLs [19]. Therefore, oligomerization of FasL improves the efficacy with which apoptosis is induced [20].

DX2, an anti-Fas monoclonal antibody of the IgG1 subclone, induces apoptosis upon cross-linking the T cell Fas receptor [21]. Cheung and Anseth [16] previously demonstrated that DX2 induces nearly 20% T cell apoptosis when covalently conjugated to the surface of gels formed from 7.5 wt% PEGDA and 2.5 wt% N-hydroxysuccinimide-PEG-acrylate (NPA) hydrogel. Others have shown a local anti-inflammatory effect mediated by IgM-class anti-Fas antibodies adsorbed to polyester membranes [22,23]. While coating anti-Fas antibody directly onto biomaterial surfaces preserves some biological activity, these strategies yield a relatively low protein surface density and limited accessibility of functional groups to the surroundings. Herein, a living radical photopolymerization (LRP)-based strategy was exploited to graft PEG chains with pendant DX2 antibodies from a polymeric surface. As illustrated in Fig. 1, an LRP mechanism is mediated by a photoiniferter specie, containing a diethyldithiocarbamate (DTC) group able to reversibly initiate photopolymerization from a surface. DTC-mediated LRP yields uniform, highly mobile polymer chains whose length is proportional to photopolymerization time [24]. As previously reported [25,26], upon covalent modification with a polymerizable acrylate group, antibodies may be co-polymerized onto these surface-anchored polymer chains. This architecture provides several benefits, including improved protein accessibility to the surroundings due to high chain mobility and increased antibody surface density due to the incorporation of multiple antibodies per chain. In addition, the natural DX2 clustering that occurs as antibodies are incorporated on polymer chains may provide the added benefit of increasing the likelihood that multiple DX2 binding events occur at one T cell Fas receptor. This multimerization could improve the chance that an apoptotic signal is delivered.

Herein, the fabrication, characterization and evaluation of surface-initiated polymer chains are reported for chains consisting of PEG monoacrylate (400 Da) with a high surface density of pendant acrylated IgG. Further, cell studies were performed to evaluate the effects of DX2-conjugating polymer coatings on inducing T cell apoptosis. Finally, a T cell adhesion ligand, Inter-Cellular Adhesion Molecule-1 (ICAM-1), was incorporated in the polymer coating to increase the interaction between T cells and the material surface. Our group has previously demonstrated that iniferter-mediated LRP allows for the fabrication of multifunctional grafts [25], and here, we report dually-functionalized polymeric coatings, containing DX2 and ICAM-1, which yield a significant increase in T cell apoptosis.

## 2. Materials and methods

### 2.1. Materials

Mouse anti-human Fas monoclonal IgG (DX2), goat anti-Fas receptor IgG, and ICAM-1/Fc chimera fusion protein (ICAM-1) were obtained from R&D Systems. All

other IgGs were obtained from Jackson ImmunoResearch. Soluble Fas receptor was purchased from Peprotech. Monoacrylated poly(ethylene glycol)-N-hydroxysuccinimide (ACRYL-PEG-NHS, MW = 3400) was purchased from Laysan Bio Inc. Slide-a-Lyzer dialysis cassettes (10,000 MWCO), Fluoraldehyde Reagent Solution, and TMB ELISA Substrate were obtained from Thermo Fisher Scientific. Aromatic urethane diacrylate (UDA) was a generous gift donated by UCB Chemicals Corp. Triethylene glycol diacrylate (TEGDA) was purchased from Polysciences Inc. Tetraethylthiuram disulfide photoiniferter (TED) was obtained from Sigma-Aldrich. 2,2-dimethoxy-2-phenylacetophenone initiator (DMPA) was purchased from Ciba Specialty Chemicals. Monoacrylated poly(ethylene glycol) (ACRYL-PEG, MW = 400) was purchased from Monomer-Polymer & Dajac Labs. Vybrant apoptosis assay kit #3, AlamarBlue reagent, and Trypan Blue stain were obtained from Invitrogen. Vector VIP stain was obtained from Vector Labs.

### 2.2. Protein acrylation and characterization

Goat IgG (IgG), fluorescein-conjugated goat IgG (F-IgG), DX2 and ICAM-1 were acrylated by reacting proteins (2 mg/ml) with 3400 Da ACRYL-PEG-NHS at defined molar ratios in 50 mM sodium bicarbonate buffer, pH 8.4. The reactions proceeded for 3 h at room temperature under constant stirring. The percentage of protein acrylation was determined immediately following reaction using Fluoraldehyde reagent to compare the concentration of free amine groups prior to and following reaction. Unreacted ACRYL-PEG-NHS was removed by dialysis against deionized water for 24 h using a 10 000 MWCO Slide-a-Lyzer dialysis cassette. Solutions were lyophilized to yield solid acrylated IgG (ACRYL-IgG), acrylated F-IgG (F-ACRYL-IgG), acrylated DX2 (ACRYL-DX2), or acrylated ICAM-1 (ACRYL-ICAM-1).

### 2.3. Preparation of the polymer substrate

The polymeric grafting substrate used in these studies consisted of 49.125 wt% UDA, 49.125 wt% TEGDA, 0.25 wt% TED iniferter, and 1.5 wt% DMPA initiator. This pre-polymer solution was sonicated and stirred intermittently for >1 h and was purged with argon for 2 min prior to polymerization. The base layer was photopolymerized by exposing mixed pre-polymer solution to 35 mW/cm<sup>2</sup> ultraviolet, collimated light generated by a mercury arc-lamp centered at 365 nm for 500 s. Sebra et al. [25] has previously demonstrated that these conditions yield a polymeric network with greater than 90% double bond conversion. Polymerized UDA-TEGDA substrates were immersed in methanol for 15 min with stirring to remove unreacted monomers and excess DMPA.

### 2.4. Surface-initiated photopolymerization of acrylated proteins

Acrylated proteins were covalently incorporated on polymer chains using a living radical photopolymerization-based chemistry as previously described [25]. Briefly, acrylated protein, including 250  $\mu$ g/ml ACRYL-IgG, 250  $\mu$ g/ml ACRYL-DX2, or 25  $\mu$ g/ml ACRYL-ICAM-1, was dissolved in 50% v/v 400 Da ACRYL-PEG in phosphate buffered saline (PBS, pH = 7.4). This solution was applied onto the DTC-containing substrate surface prepared as described earlier and exposed to 35 mW/cm<sup>2</sup> collimated ultraviolet light centered at 365 nm for 0–900 s. Following polymerization, devices were immersed in deionized water for 1 h, followed by rinsing in 70% ethanol overnight. Then, the devices were washed in sterile-filtered 30% ethanol for 1 h and finally rinsed in sterile PBS overnight. All washing steps were carried out at room temperature with mixing.

### 2.5. Detection of polymerized ACRYL-IgG

The surface density of polymerized ACRYL-IgG was assessed using a modified ELISA. ACRYL-IgG coatings were incubated at room temperature for 8 min with 8  $\mu$ g/ml horse radish peroxidase (HRP)-conjugated donkey anti-goat detection antibody (HRP-DAG-IgG), and then rinsed 4 times with PBS. HRP-treated coatings were either: (1) Incubated 15 min with Vector VIP reagent to stain HRP, or (2) Dissected with a biopsy punch into 6 mm diameter disks and placed in the bottom of a 96-well plate. These HRP-treated samples were incubated with 100  $\mu$ l TMB ELISA substrate for 20 min with mixing to allow color change, and the reaction was quenched with the addition of 100  $\mu$ l 2 N H<sub>2</sub>SO<sub>4</sub>. The 450 nm absorbance of each sample was measured and converted to ACRYL-IgG surface density by comparing sample absorbance to that of TMB-treated control solutions with known HRP-DAG-IgG mass.

Fluorescein-conjugated ACRYL-goat IgG (F-ACRYL-IgG) was polymerized, as described above, and incubated 30 min with 8  $\mu$ g/ml rhodamine-conjugated donkey anti-goat IgG (R-DAG-IgG) prior to fluorescent imaging with confocal microscopy (Axioplan 2, Zeiss). Height of dry coatings was determined using profilometry (Stylus Profiler, Dektak 6M, force = 1 mg, radius = 12.5 mm, and range = 1 mm).

### 2.6. Characterization of ACRYL-DX2-containing coatings

ACRYL-DX2 was photografted at a concentration of 250  $\mu$ g/ml, as described above. Grafted ACRYL-DX2 was detected and quantified by Vector VIP staining and the modified ELISA described above, where an HRP-conjugated goat anti-mouse

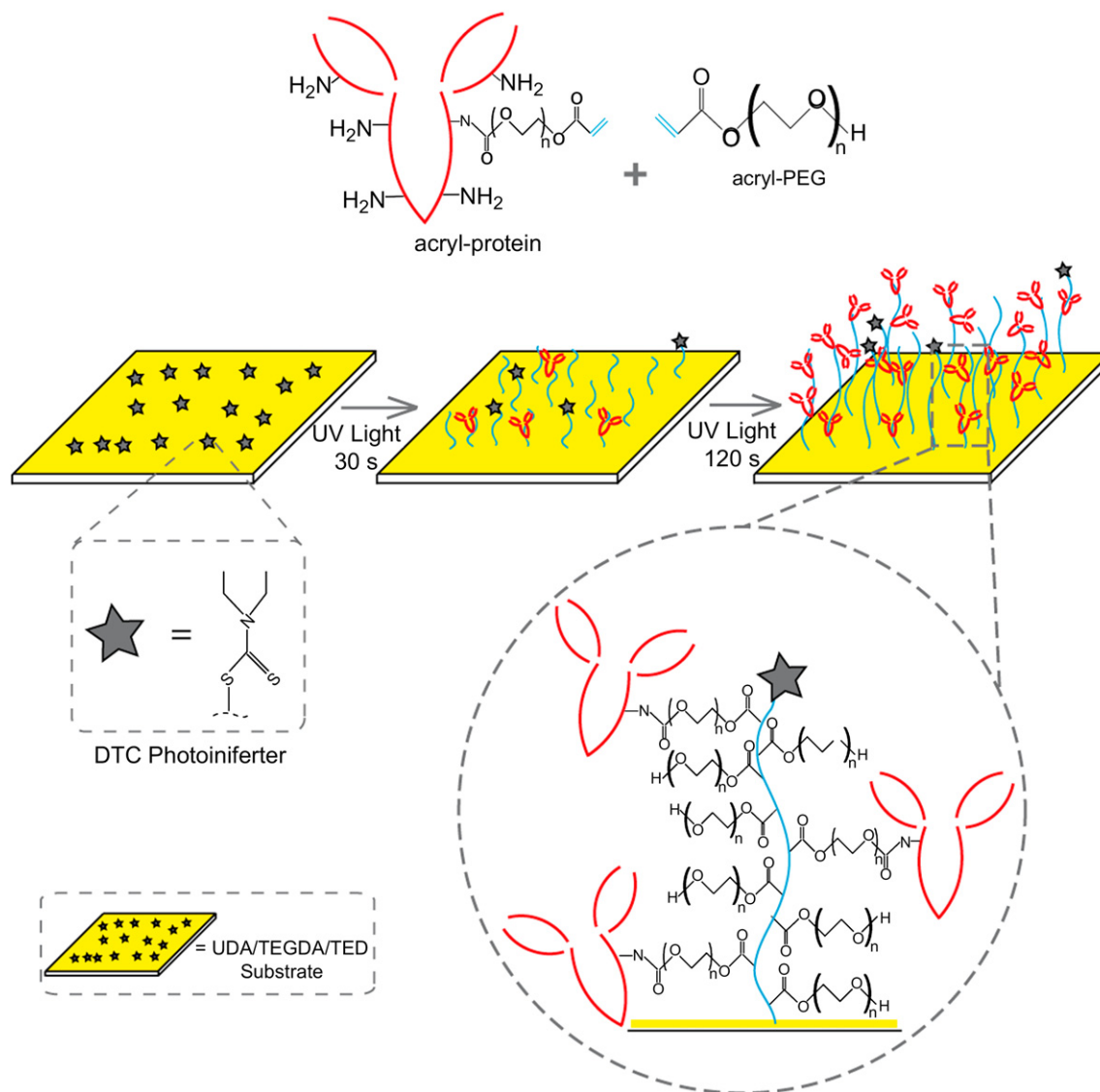


**Fig. 1.** Schematic illustrating surface-initiated polymerization of acrylated proteins. ACRYL-protein is co-photopolymerized with ACRYL-PEG atop a polymeric substrate containing a DTC photoiniferter. Polymer chains consisting of polyacrylate backbones with pendant proteins are formed on the surface, and the surface modification is proportional to UV exposure time.

IgG (HRP-GAM-IgG) was used as the detection antibody. In addition, a modified sandwich ELISA was performed where devices containing polymerized ACRYL-DX2 were incubated for 1 h with 1  $\mu$ g/ml soluble Fas receptor, followed by 1  $\mu$ g/ml goat anti-Fas receptor IgG, and incubated 8 min with 5  $\mu$ g/ml HRP-DAG-IgG. Samples were rinsed and stained with Vector VIP for 15 min to verify ACRYL-DX2 maintained the capacity to bind the Fas receptor following incorporation in the surface graft.

### 2.7. Cell culture

Jurkat T cell lymphoma cells and 19.2 Fas-insensitive Jurkats (ATCC, Manassas, VA) were cultured in RPMI 1640 supplemented with 10% fetal bovine serum, 100  $\mu$ g/ml Penicillin/Streptomycin, and 0.5  $\mu$ g/ml Fungizone. Cells were incubated at 37 °C in humid conditions with 5% CO<sub>2</sub>. The biological activity of soluble ACRYL-DX2 was assessed by incubating Jurkat T cells (50 000 cells/ml, 200  $\mu$ l media) with ACRYL-DX2 at a concentration of 5  $\mu$ g/ml. After 6, 12, 24, and 48 h, the percentage of T cells undergoing apoptosis was analyzed using an Annexin assay, as described below. Maximum T cell apoptosis was detected after 24 h of culture with ACRYL-DX2, so this time point was used for all subsequent studies. The biological activity of functionalized polymer coatings containing ACRYL-DX2 was also evaluated by incubation with T cells. Disks of functionalized substrate were dissected using a 6 mm diameter biopsy punch and placed in the bottom of a 96-well plate. Jurkat and 19.2 T cells were seeded atop coatings at 50 000 cells/ml in 200  $\mu$ l media and cultured for 24 h, prior to analysis for apoptosis.

### 2.8. T cell assays

T cells were stained for apoptosis using the Vybrant apoptosis assay kit #3. Cells were stained with fluorescein-labeled Annexin V and counterstained with propidium iodide (PI) to differentiate apoptotic and necrotic cells, respectively. Cells were imaged using a Nikon Eclipse TE300 fluorescent microscope and counted in 4 random fields of view per sample. Each field contained approximately 100–200 cells. The fraction of apoptotic cells was calculated by dividing the number of fluorescein-positive (but PI-negative) T cells by the cell number. Bulk T cell metabolic activity was also analyzed after 24 h by adding 22  $\mu$ l of AlamarBlue reagent to each condition (resulting in a 10% v/v AlamarBlue solution) and incubating for 3 h. Fluorescence (excitation: 560 nm, emission: 590 nm) represented the metabolic activity of the living cells. All cell data is shown as the mean of 4 replicates and each experiment has been repeated at least twice.

### 2.9. T-cell adhesion studies

T cells were seeded atop coatings functionalized with ACRYL-ICAM-1, ACRYL-DX2, ACRYL-ICAM-1/ACRYL-DX2, or control, in 96-well plates, as described above. At 6 h, 12 h, and 24 h time points, media was removed from each well and gently washed three times with 200  $\mu$ l PBS. 50  $\mu$ l of 50% Trypan Blue stain (0.4%), 50% media was added to denote dead cells and incubated 5 min. Bright field microscopy was used to count the number of live cells remaining on the polymer surface and the percentage of adherent cells was calculated by dividing the number of cells remaining on the polymer surface by the total number of cells seeded.

## 2.10. Statistical analysis

Statistical significance was determined using a two-tailed, unpaired Student's *t*-test. Differences between datasets were considered statistically significant when the *p* value was less than 0.05. All results are presented as mean  $\pm$  standard error of the mean.

## 3. Results

### 3.1. Acrylation of IgG

IgG was acrylated prior to surface grafting by reacting primary amine groups with ACRYL-PEG-NHS. Degree of acrylation was controlled by varying the molar ratio of ACRYL-PEG-NHS to IgG from 0:1 to 25:1. While increasing the number of acrylate groups per IgG increases the likelihood that the protein will be incorporated into graft polymer chains, over-modification can reduce the biological activity of the molecule. To verify the biological activity of ACRYL-DX2 (acrylated anti-Fas IgG) post modification, ACRYL-DX2 was added to Jurkat T cell cultures for 24 h to induce apoptosis. As shown in Fig. 2, a 25-fold, but not 10-fold, molar excess of ACRYL-PEG-NHS to DX2 resulted in a significant reduction in biological activity. Thus, a reaction ratio of 10 moles ACRYL-PEG-NHS per mole IgG was used for all future studies. A Fluoraldehyde assay indicated these reaction conditions yielded  $2.2 \pm 0.6\%$  acrylation of this 150 kDa IgG.

### 3.2. Surface grafting of acrylated IgG

As illustrated in Fig. 1, ACRYL-IgG was dissolved in 50% ACRYL-PEG (400 Da) in PBS and photopolymerized from an iniferter-containing UDA-TEGDA substrate for controlled polymerization times ranging from 0 to 900 s. Because of the LRP nature of this system, one expects the polymer thickness and ACRYL-IgG incorporation to increase proportionally to light exposure time. As shown in Fig. 3A, profilometry of dry grafts revealed increasing dry polymer height with UV exposure time. Fig. 3B illustrates the relationship between detectable ACRYL-IgG surface density with photopolymerization time. Unlike dry graft height, detectable ACRYL-IgG did not consistently increase with time. Instead, a peak in detectable ACRYL-IgG existed between 120 and 180 s. ACRYL-IgG surface density was determined by a modified ELISA, so incorporated protein was only observable if bound by a detection antibody (150 kDa). We postulate that the surface-initiated chains become

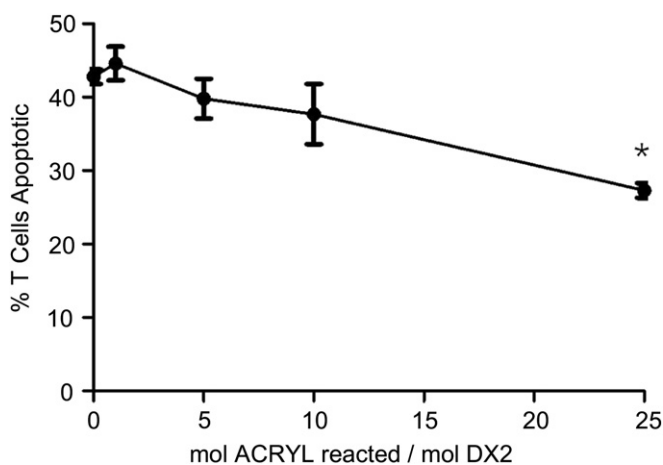


**Fig. 2.** The influence of covalent acrylation on the bioactivity of soluble ACRYL-DX2. ACRYL-PEG-NHS was reacted with DX2 in the molar ratios shown on the *x*-axis. As the reaction stoichiometry was increased, the efficacy with which soluble ACRYL-DX2 induced apoptosis was reduced.

cross-linked for polymerization times greater than 180 s due to chain transfer and other non-idealities, so the detection antibody was unable to penetrate deeply into the coating. Further evidence of this phenomenon is presented below.

### 3.3. Surface grafting of fluorescent ACRYL-IgG

Fluorescein-tagged ACRYL-IgG (F-ACRYL-IgG) was photografted for either 150 or 500 s. As seen in the cross-sectional images of surface-initiated coatings, shown in Fig. 3C, fluorescein was visible throughout the full thickness for 150 and 500 s polymerization times. Swollen coatings were approximately 10  $\mu$ m and 25  $\mu$ m thick, respectively. Following fabrication, surfaces were incubated with rhodamine-tagged donkey anti-goat IgG (R-IgG) to selectively label the accessible F-ACRYL-IgG. As seen in Fig. 3D, strong rhodamine fluorescence is visible throughout the full thickness of the 150 s graft but only observed near the top of the 500 s graft. Control coatings lacking F-ACRYL-IgG revealed no significant fluorescein or rhodamine fluorescence (data not shown), demonstrating that the presence of fluorescence is due to F-ACRYL-IgG and specific antibody binding, and not the result of physical entrapment of the antibodies. Coupled with the spike in detectable antibody observed between 120 and 180 s, we believe that the 150 and 500 s fluorescence profiles provide insight into the architecture of this surface-initiated polymer network. We postulate that non-idealities in polymer chain formation, likely due to chain transfer events, result in chain cross-linking during longer polymerization times (>300 s). This cross-linking prevents the diffusion of 150 kDa R-IgG through graft chains and indicates that ACRYL-IgG incorporated early during the surface modification is inaccessible to the outside environment. To ensure a high surface density of accessible ACRYL-IgG, a photopolymerization time of 150 s was used for all future studies.

### 3.4. Iniferter concentration and ACRYL-IgG surface density

Surface modification and coating properties are further controlled by the density of surface grafting sites. The effect of iniferter concentration on detectable ACRYL-IgG was studied by varying the initial concentration of TED in the pre-polymer solution from 0.25 to 1.0 wt% and subsequent grafting of ACRYL-IgG for 150 s. As shown in Fig. 3E, maximum detectable ACRYL-IgG surface densities were observed at the lowest TED concentration, 0.25 wt%. Because TED concentration correlates with the surface-bound DTC concentration, lowering the concentration of TED in the substrate reduces the total number of polymer chains initiated from the surface. By decreasing the total surface density of polymer chains, it is likely that the resulting polymer chains gain greater mobility, increasing the overall accessibility of incorporated ACRYL-IgG, and minimizes network formation via cross-linking. Minimal polymer chain initiation occurred for TED concentrations below 0.25 wt%, so lower TED concentrations were not investigated.

### 3.5. T cell apoptosis by grafted ACRYL-DX2

ACRYL-DX2 was incorporated into surface-anchored polymer chains using the photopolymerization conditions identified to yield a high protein surface density (150 s photopolymerization, 0.25 wt% TED). Polymers were washed >36 h, as described above, to remove any unconjugated ACRYL-DX2. Incorporation of ACRYL-DX2 was verified using an ELISA-type assay and was consistently found to be between 1.4 and 1.7 ng/cm<sup>2</sup>. Additionally, Vector VIP staining was performed prior to each ACRYL-DX2 cell experiment to verify the presence of anti-Fas IgG. The staining of circular-patterned ACRYL-DX2 grafts, shown in Fig. 4A, confirms the

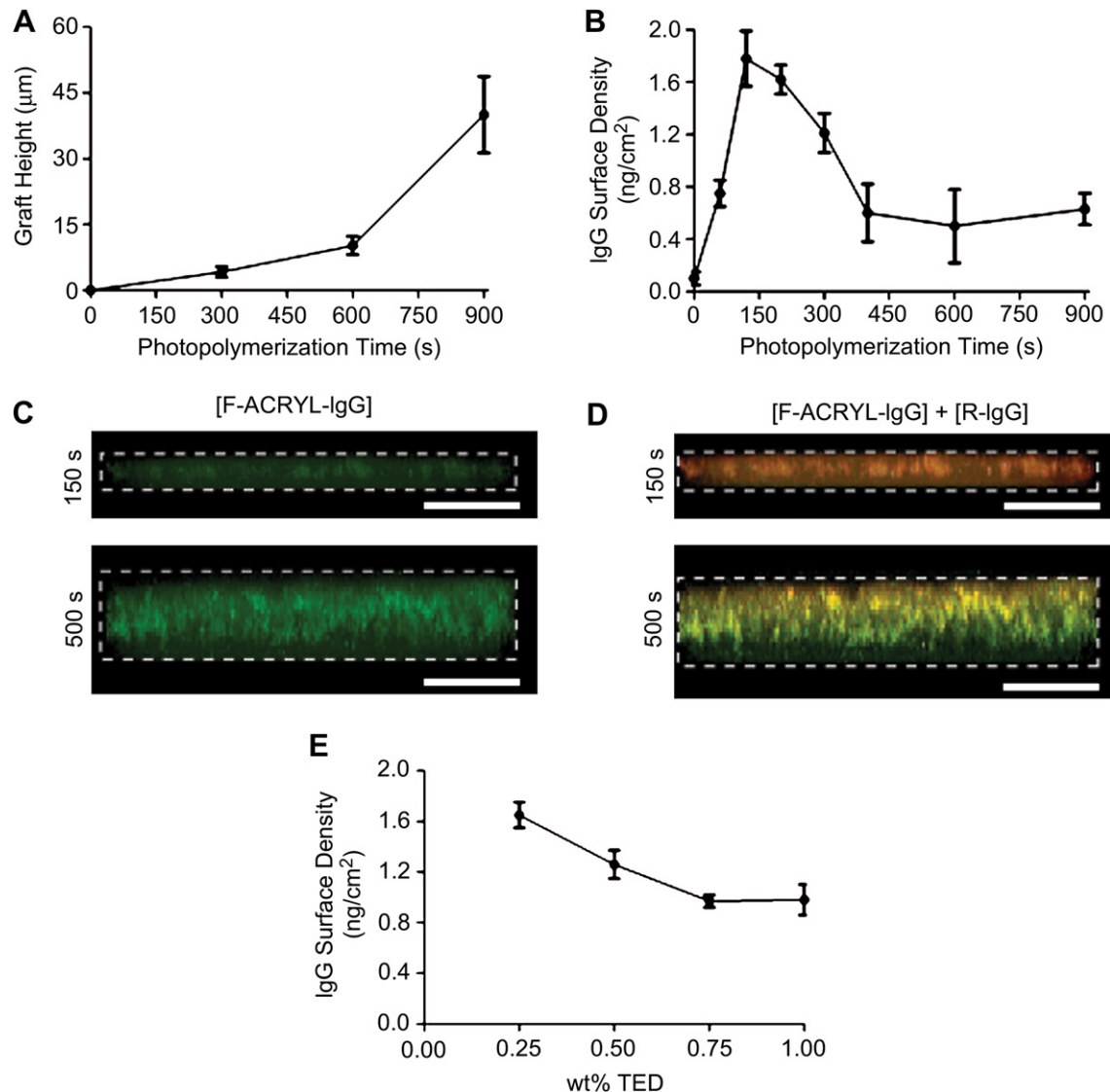


**Fig. 3.** Controlled surface-initiated photopolymerization of ACRYL-IgG. (A) Dry graft height, determined by profilometry, increases as a function of surface-initiated polymerization time. (B) Surface density of detectable ACRYL-IgG increases and then decreases as a function of polymerization time, as determined by modified ELISA. A region of high detectable ACRYL-IgG exists between 120 and 180 s fabrication times. (C) Fluorescein-tagged ACRYL-IgG from goat (F-ACRYL-IgG) was photografted for 150 and 500 s. Dashed boxes represent a cross-sectional view of the full thickness of each coating. Fluorescein is visible throughout the thickness of both samples. Scale bars = 50  $\mu\text{m}$ . (D) F-ACRYL-IgG Grafts were stained with rhodamine-tagged donkey anti-goat IgG (R-IgG) to label accessible F-ACRYL-IgG. Strong full thickness R-IgG staining is visible at 150 s but only surface staining at 500 s. Scale bars = 50  $\mu\text{m}$ . (E) Surface density of detectable ACRYL-IgG decreased as a function of TED iniferter concentration in the substrate.

presence of ACRYL-DX2 (left) and that grafted ACRYL-DX2 remains specific binding ability to Fas receptor (right).

The biological activity of polymerized ACRYL-DX2 was assessed by its ability to induce apoptosis in T cells. Jurkat T cells were seeded onto surfaces with or without ACRYL-DX2 for 24 h. Apoptotic cells were stained with fluorescein-conjugated Annexin V. Fig. 4B shows representative fluorescent images of apoptotic Jurkat T cells on a control surface, while Fig. 4C illustrates an increase in Jurkat apoptosis when seeded on a surface containing ACRYL-DX2. As shown in Fig. 4D, ACRYL-DX2 surfaces induced significant apoptosis,  $21 \pm 2\%$  of Jurkat T cells. When 19.2 T cells (Jurkats rendered insensitive to Fas-mediated apoptosis [27,28]) were exposed to ACRYL-DX2 grafts, no significant increase in apoptosis was observed. This indicates that the apoptosis induced by grafted ACRYL-DX2 is specific and mediated through DX2/Fas signaling.

### 3.6. Apoptosis by grafted ACRYL-ICAM-1 and ACRYL-DX2

We chose to incorporate a 70 kDa ICAM-1/Fc fusion protein because its structural similarity to IgG allowed predictable acrylation using the same conditions identified for ACRYL-IgG. ACRYL-ICAM-1 and ACRYL-DX2 were simultaneously co-polymerized from the iniferter-containing substrates, as Sebra et al. [25] has previously demonstrated that multiple acrylated proteins may be simultaneously polymerized with the LRP grafting technique. As shown in Fig. 5A, seeding T cells on grafted polymer surfaces functionalized with ACRYL-DX2 and ACRYL-ICAM-1 resulted in  $34 \pm 1\%$  Jurkat T cell apoptosis, an improvement of nearly 50% when compared to ACRYL-DX2 alone. Surfaces functionalized with only ACRYL-ICAM-1 did not yield a significant increase in apoptosis relative to controls, demonstrating a synergistic effect between ACRYL-ICAM-1 and ACRYL-DX2. Culturing Jurkats on ACRYL-DX2/ACRYL-ICAM-1 functionalized

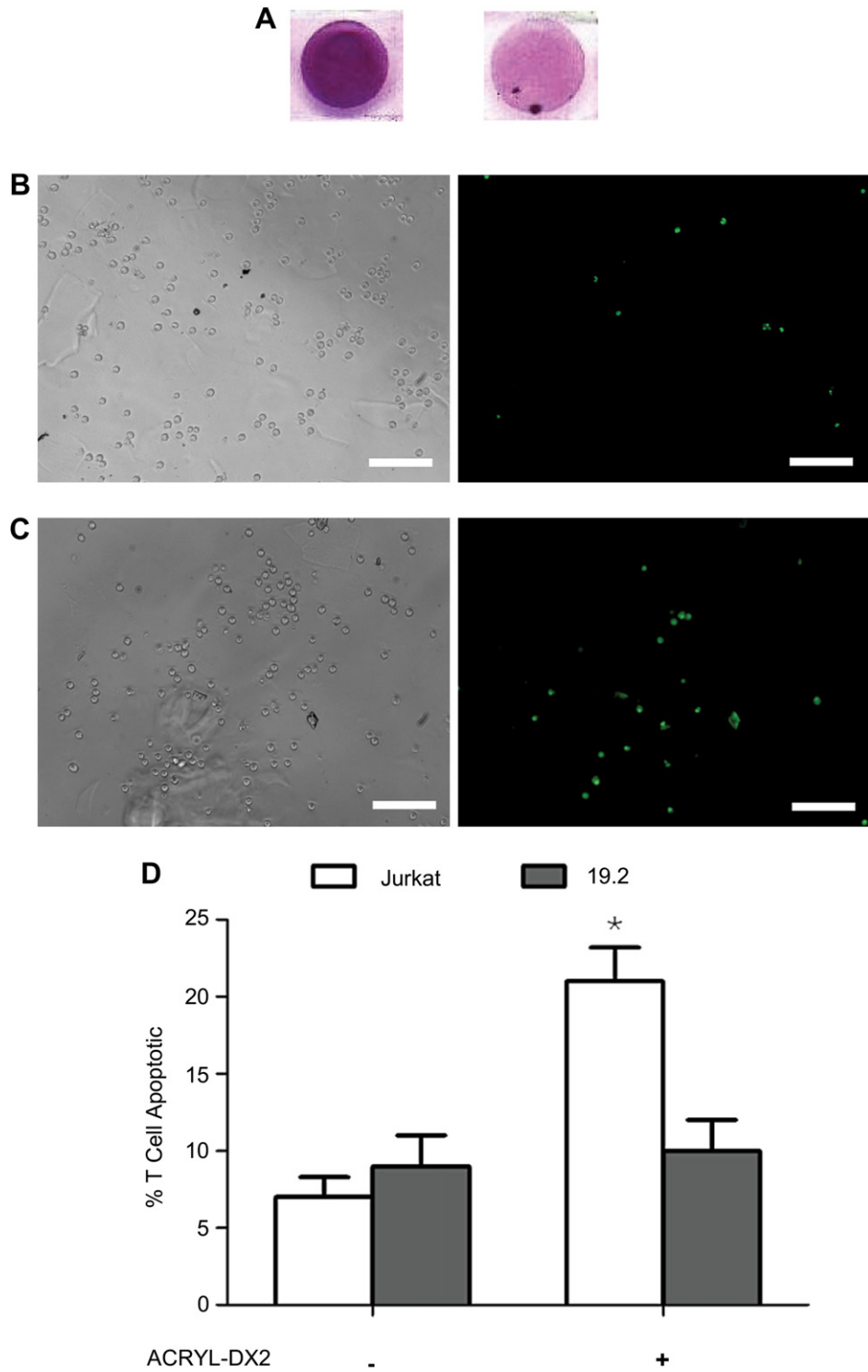


**Fig. 4.** Grafted ACRYL-DX2 induces T cell apoptosis. (A) ACRYL-DX2 was incorporated in 6 mm diameter grafts and incubated with HRP-conjugated GAM IgG (left) or soluble Fas receptor, goat anti-Fas IgG, and HRP-conjugated DAG IgG (right). Both (left) and (right) were stained with Vector VIP to stain HRP. Vector VIP staining indicates (left) high ACRYL-DX2 surface density and (right) ACRYL-DX2 retains the ability to bind the Fas receptor. (B & C) Representative bright field (right) and 480 nm fluorescent (left) images of Jurkat T cells seeded for 24 h on grafted (B) control and (C) ACRYL-DX2 surfaces for 24 h followed by staining with fluorescein-conjugated Annexin V. Apoptotic T cells are visible at 480 nm. Scale bars = 100  $\mu$ m (D) Jurkat and Fas-insensitive 19.2 T cells were seeded on grafted surfaces for 24 h and assayed for apoptosis. A statistically significant increase in apoptosis was observed for Jurkat T cells incubated on ACRYL-DX2 surfaces. Asterisks indicate a statistically significant difference ( $p < 0.05$ ) from all other values.

surfaces demonstrated more than a 50% reduction in metabolic activity when compared to control surfaces (Fig. 5B), likely due to a reduction in the number of living T cells. A statistically significant reduction in metabolic activity was not observed for T cells cultured on polymeric surfaces functionalized singularly with either ACRYL-

DX2 or ACRYL-ICAM-1, highlighting the importance of the synergistic effect between ACRYL-ICAM-1 and ACRYL-DX2 in reducing the population of T cells. No increase in apoptosis or decrease in metabolic activity was observed for 19.2 cells, indicating these effects were Fas-mediated.

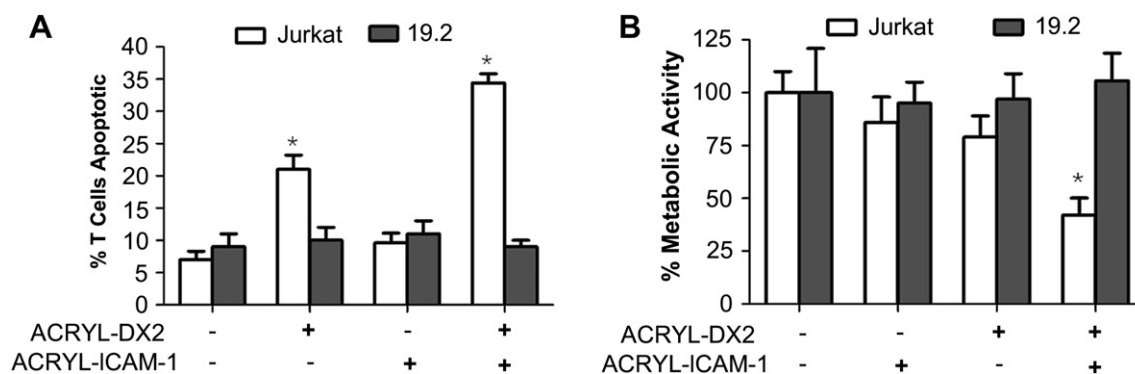


**Fig. 5.** ACRYL-ICAM-1 improves the efficacy of grafted ACRYL-DX2. (A) Grafted ACRYL-ICAM-1, when incorporated with ACRYL-DX2, increases the percentage of Jurkat T cells signaled to undergo apoptosis after 24 h. (B) Metabolic activity studies of Jurkat T cells seeded on control or dually-functionalized grafted surfaces for 24 h. Jurkat T-cells show an over 50% reduction in metabolic activity when cultured on ACRYL-DX2/ACRYL-ICAM-1 grafts. Asterisks indicate a statistically significant difference ( $p < 0.05$ ) from all other values.

### 3.7. Probing the T cell/material interaction

When incorporating ACRYL-ICAM-1, we considered the possibility that this ligand could enable T cells to form sustained adhesions with the functionalized surface. This behavior might be deleterious to the end goal of immunoprotection, as lymphocyte recruitment could increase the local concentration of inflammatory cytokines. T cell adherence was analyzed at 6 h, 12 h, and 24 h following seeding on polymers functionalized with ACRYL-ICAM-1 and/or ACRYL-DX2. At all time points, less than 1% of cells seeded upon the polymer surface remained following a wash to remove non-adherent cells.

## 4. Discussion

Towards protecting allograft tissue from rejection, cell encapsulation strategies continue to improve. Despite improvements, however, T cell-mediated rejection continues to pose a considerable hurdle to transplant acceptance. This work aimed to fabricate biomaterial coatings to reduce the local concentration of T cells. Towards that end, we utilized an iniferter-based LRP to fabricate functionalized coatings, which mimic *in vivo* T cell signaling events.

IgG was covalently modified with acrylate groups and subsequently polymerized into surface-imitated polymer chains of poly(ethylene glycol). Using this polymer chemistry, maximum detectable IgG concentrations were identified for photopolymerization times ranging from 120 to 180 s, indicating that polymer networks became cross-linked for polymerization times greater than 180 s, and therefore, were less accessible to the surrounding environment. This notion was supported by the observation that fluorescently-labeled secondary antibody was able to penetrate throughout a  $\sim 20 \mu\text{m}$  coating generated by 150 s UV light exposure, but was unable to diffuse deeply within a  $\sim 50 \mu\text{m}$  coating generated by a 500 s exposure. Network cross-linking was likely the result of polymer chain transfer, and other non-idealities, which become more apparent with increased photopolymerization time. Even though polymerized fluorescent IgG was visible throughout polymer coatings grafted for 150 and 180 s, it is reasonable to assume that polymerized IgG which was not detectable by a secondary IgG would also be inaccessible to T cells. Thus, in keeping with the goal of fabricating a coating that allows bioactive molecules to be highly accessible to nearby cells, a polymerization time of 150 s was used for all future studies.

Utilizing the appropriate fabrication conditions identified for grafting ACRL-IgG, Anti-Fas IgG (ACRYL-DX2) was incorporated into the polymer network. When T cells were seeded atop ACRYL-DX2-functionalized coatings for 24 h, significant apoptosis ( $21 \pm 2\%$  of

cells) was observed. Prior to incubation with T cells, coatings were rinsed for 36 h, as described earlier, to allow for the complete removal of non-covalently incorporated ACRYL-DX2. Therefore, the observed increase in apoptosis is due to surface-bound ACRYL-DX2, and not soluble DX2. While T cell apoptosis induced by this ACRYL-DX2-functionalized surface represents only a modest increase over the level of apoptosis induced by a previously described system, consisting of a hydrogel coated with DX2 [16], it is critical to note that our LRP grafting approach requires 80% less DX2 than the previously-investigated hydrogel coating.

While PEG is an important component of the surface-mediated polymerization, PEG is also known as a chemistry that resists non-specific protein interactions, thereby rendering it minimally adhesive for most cell types. Thus, we postulated that increased T cell apoptosis might be achieved by introducing an Inter-cellular Adhesion Molecule-1 (ICAM-1), a member of the immunoglobulin superfamily, into an ACRYL-DX2-functionalized polymeric surface. ICAM-1 is expressed by selected cell types, including endothelial cells and antigen presenting cells (APCs), and is known to bind a  $\beta 2$ -integrin, Leukocyte Functional Antigen-1 (LFA-1), expressed on the T cell surface [29]. ICAM-1 binding is essential to initiating several T cell attachment mechanisms, including adhesion to endothelial cells for transmigration through blood vessel wall in addition to the formation of the immune synapse with an APC [29]. Furthermore, ICAM-1 binding has been shown to enhance the activity of membrane-bound FasL. Sieg et al. blocked ICAM-1 on the surface of FasL-expressing effector cells and observed a significant decrease in T cell apoptosis induction, suggesting that LFA-1/ICAM-1 binding stabilizes the adhesion between target and effector cells during Fas/FasL signaling [30].

Fig. 5 shows that the addition of acrylated ICAM-1 significantly increases ( $>50\%$ ) the apoptosis induced by an ACRYL-DX2-functionalized coating and significantly decreased ( $<50\%$ ) the overall T cell metabolic activity. Further, T cell adhesion studies indicate that this effect was possible without long-term, stable adhesion between T cells and the biomaterial surface. This is likely possible because the interaction between T cells and ICAM-1 is short lived. Others have investigated the transient nature of the interaction between T cells and ICAM-1-coated surfaces. For example, Somersalo et al. reported that T cells formed stable adhesions to ICAM-1-coated surfaces for approximately 15 min before releasing [31]. Fortunately, the induction of Fas-mediated apoptosis occurs quickly [32], and our results indicate that the transient increase in adhesion afforded by ICAM-1 is sufficient to significantly increase ACRYL-DX2-mediated apoptosis. Further, the observed lack of sustained adhesion provides encouragement that this coating could

avoid significant lymphocyte recruitment, minimizing the local concentration of inflammatory cytokines.

As with any biomaterial developed towards the eventual goal of implantation, it is important to consider the competing effects that this coating might have upon cell types not investigated herein. This is particularly important because, in addition to T cells, ICAM-1 is known to bind several classes of leukocytes. For example, ICAM-1 is implicated in neutrophil transendothelial migration [33,34] and macrophage adherence [35,36]. While the interaction that neutrophils and macrophages might have with an ICAM-1-coated biomaterial surface has not been well studied, some interaction between these cells and a coating functionalized with ACRYL-DX2/ACRYL-ICAM-1 might ultimately be beneficial towards the goal of immunoprotection. This is because, like T cells, neutrophils and macrophages have been shown to undergo apoptosis in response to Fas receptor stimulation [22,23,37–39]. Thus, the anti-inflammatory benefits of an ACRYL-DX2/ACRYL-ICAM-1-functionalized surface could extend beyond T cells, offering greater promise that this coating may provide an active barrier against transplant rejection.

## 5. Conclusion

A surface-initiated polymerization was utilized to grow polymer chains containing anti-Fas antibody and ICAM-1 from a polymeric substrate to induce significant T cell apoptosis. Appropriate surface-mediated photopolymerization conditions were identified to polymerize a high density of detectable acrylated protein. Surfaces with polymerized ACRYL-DX2 were shown to illicit Fas-mediated T cell apoptosis, and the addition of a T cell adhesion ligand, ACRYL-ICAM-1, enhanced this pro-apoptotic affect. These findings indicate that dually-functionalized (DX2 & ICAM-1) surfaces are capable of significantly reducing the local T cell population. In summary, this study introduces a new methodology to functionalize polymeric surfaces with immunosuppressive proteins and this graft architecture offers potential as a bioactive coating for future cell encapsulation devices.

## Acknowledgements

The authors wish to thank Dr. Charles Cheung for training and initial guidance in this project, Dr. Chien-Chi Lin for helpful discussions regarding several aspects of this work and Dr. McKinley Lawson for training with surface-initiated polymerization. Additionally, the authors thank Mark Tibbitt and Cole DeForest for assistance with profilometry and imaging, respectively. The authors gratefully acknowledge financial support from the National Institute of Health (R01DK076084), the Howard Hughes Medical Institute, and the Department of Education's Graduate Assistance in Areas of National Need for a fellowship to PSH.

## Appendix

Figures with essential color discrimination. Certain figures in this article, in particular Figs. 1 and 4, have parts that are difficult to interpret in black and white. The full color images can be found in the on-line version, at doi:10.1016/j.biomaterials.2010.01.035.

## References

- [1] Wollert KC, Drexler H. Cell-based therapy for heart failure. *Curr Opin Cardiol* 2006;21(3):234–9.
- [2] Emerich DF, Winn SR. Immunoisolation cell therapy for CNS diseases. *Crit Rev Ther Drug Carrier Syst* 2001;18(3):265–98.
- [3] Lee MK, Bae YH. Cell transplantation for endocrine disorders. *Adv Drug Deliv Rev* 2000;42(1–2):103–20.
- [4] Wilson JT, Chaikof EL. Challenges and emerging technologies in the immunoisolation of cells and tissues. *Adv Drug Deliv Rev* 2008;60(2):124–45.
- [5] Lim F, Sun AM. Microencapsulated islets as bioartificial endocrine pancreas. *Science* 1980;210(4472):908–10.
- [6] Kabelitz D, Geissler EK, Soria B, Schroeder IS, Fandrich F, Chatenoud L. Toward cell-based therapy of type 1 diabetes. *Trends Immunol* 2008;29(2):68–74.
- [7] de Vos P, Marchetti P. Encapsulation of pancreatic islets for transplantation in diabetes: the untouchable islets. *Trends Mol Med* 2002;8(8):363–6.
- [8] Mandrup-Poulsen T, Zumsteg U, Reimers J, Pociot F, Morch L, Helqvist S, et al. Involvement of interleukin 1 and interleukin 1 antagonist in pancreatic beta-cell destruction in insulin-dependent diabetes mellitus. *Cytokine* 1993;5(3):185–91.
- [9] Jang JY, Lee DY, Park SJ, Byun Y. Immune reactions of lymphocytes and macrophages against PEG-grafted pancreatic islets. *Biomaterials* 2004;25(17):3663–9.
- [10] Lee DY, Park SJ, Lee S, Nam JH, Byun Y. Highly poly(ethylene) glycolylated islets improve long-term islet allograft survival without immunosuppressive medication. *Tissue Eng* 2007;13(8):2133–41.
- [11] Cui H, Tucker-Burden C, Cauffiel SM, Barry AK, Iwakoshi NN, Weber CJ, et al. Long-term metabolic control of autoimmune diabetes in spontaneously diabetic nonobese diabetic mice by nonvascularized microencapsulated adult porcine islets. *Transplantation* 2009;88(2):160–9.
- [12] Yun Lee D, Hee Nam J, Byun Y. Functional and histological evaluation of transplanted pancreatic islets immunoprotected by PEGylation and cyclosporine for 1 year. *Biomaterials* 2007;28(11):1957–66.
- [13] Cheung CY, McCartney SJ, Anseth K. Synthesis of polymerizable superoxide dismutase mimetics to reduce reactive oxygen species damage in transplanted biomedical devices. *Adv Funct Mater* 2008;18:3119–26.
- [14] Leung A, Lawrie G, Nielsen LK, Trau M. Synthesis and characterization of alginate/poly-L-ornithine/alginate microcapsules for local immunosuppression. *J Microencapsul* 2008;25(6):387–98.
- [15] Lin CC, Metters AT, Anseth KS. Functional PEG-peptide hydrogels to modulate local inflammation induced by the pro-inflammatory cytokine TNFalpha. *Biomaterials* 2009;30(28):4907–14.
- [16] Cheung CY, Anseth KS. Synthesis of immunoisolation barriers that provide localized immunosuppression for encapsulated pancreatic islets. *Bioconjug Chem* 2006;17(4):1036–42.
- [17] Palmer E. Negative selection—clearing out the bad apples from the T-cell repertoire. *Nat Rev Immunol* 2003;3(5):383–91.
- [18] Nagata S, Golstein P. The Fas death factor. *Science* 1995;267(5203):1449–56.
- [19] Siegel RM, Frederiksen JK, Zacharias DA, Chan FK, Johnson M, Lynch D, et al. Fas preassociation required for apoptosis signaling and dominant inhibition by pathogenic mutations. *Science* 2000;288(5475):2354–7.
- [20] Holler N, Tardivel A, Kovacsovic-Bankowski M, Hertig S, Gaide O, Martinon F, et al. Two adjacent trimeric Fas ligands are required for Fas signaling and formation of a death-inducing signaling complex. *Mol Cell Biol* 2003;23(4):1428–40.
- [21] Cifone MG, De Maria R, Roncaioli P, Rippon MR, Azuma M, Lanier LL, et al. Apoptotic signaling through CD95 (Fas/Apo-1) activates an acidic sphingomyelinase. *J Exp Med* 1994;180(4):1547–52.
- [22] Moreno JB, Margraf S, Schuller AM, Simon A, Moritz A, Scholz M. Inhibition of neutrophil activity in cardiac surgery with cardiopulmonary bypass: a novel strategy with the leukocyte inhibition module. *Perfusion* 2004;19(1):11–6.
- [23] Scholz M, Simon A, Berg M, Schuller AM, Hacibayramoglu M, Margraf S, et al. In vivo inhibition of neutrophil activity by a FAS (CD95) stimulating module: arterial in-line application in a porcine cardiac surgery model. *J Thorac Cardiovasc Surg* 2004;127(6):1735–42.
- [24] Otsu T. Iniferter concept and living radical polymerization. *J Polym Sci Part A: Polym Chem* 2000;38(12):2121–36.
- [25] Sebra RP, Masters KS, Bowman CN, Anseth KS. Surface grafted antibodies: controlled architecture permits enhanced antigen detection. *Langmuir* 2005;21(24):10907–11.
- [26] Sebra RP, Masters KS, Cheung CY, Bowman CN, Anseth KS. Detection of antigens in biologically complex fluids with photografted whole antibodies. *Anal Chem* 2006;78(9):3144–51.
- [27] Juo P, Kuo CJ, Yuan J, Blenis J. Essential requirement for caspase-8/FLICE in the initiation of the Fas-induced apoptotic cascade. *Curr Biol* 1998;8(18):1001–8.
- [28] Juo P, Woo MS, Kuo CJ, Signorelli P, Biemann HP, Hannun YA, et al. FADD is required for multiple signaling events downstream of the receptor Fas. *Cell Growth Differ* 1999;10(12):797–804.
- [29] Dustin ML, Bivona TG, Phillips MR. Membranes as messengers in T cell adhesion signaling. *Nat Immunol* 2004;5(4):363–72.
- [30] Sieg S, Smith D, Kaplan D. Differential activity of soluble versus cellular Fas ligand: regulation by an accessory molecule. *Cell Immunol* 1999;195(2):89–95.
- [31] Somersalo K, Anikeeva N, Sims TN, Thomas VK, Strong RK, Spies T, et al. Cytotoxic T lymphocytes form an antigen-independent ring junction. *J Clin Invest* 2004;113(1):49–57.
- [32] Weis M, Schlegel J, Kass GE, Holmstrom TH, Peters I, Eriksson J, et al. Cellular events in Fas/APO-1-mediated apoptosis in JURKAT T lymphocytes. *Exp Cell Res* 1995;219(2):699–708.
- [33] Yang L, Froio RM, Sciuto TE, Dvorak AM, Alon R, Luscinskas FW. ICAM-1 regulates neutrophil adhesion and transcellular migration of TNF-alpha-activated vascular endothelium under flow. *Blood* 2005;106(2):584–92.

- [34] Smith CW, Marlin SD, Rothlein R, Toman C, Anderson DC. Cooperative interactions of LFA-1 and Mac-1 with intercellular adhesion molecule-1 in facilitating adherence and transendothelial migration of human neutrophils in vitro. *J Clin Invest* 1989;83(6):2008–17.
- [35] Simms MG, Walley KR. Activated macrophages decrease rat cardiac myocyte contractility: importance of ICAM-1-dependent adhesion. *Am J Phys* 1999; 277(1 Pt 2):H253–60.
- [36] Patel SS, Thiagarajan R, Willerson JT, Yeh ET. Inhibition of alpha4 integrin and ICAM-1 markedly attenuate macrophage homing to atherosclerotic plaques in ApoE-deficient mice. *Circulation* 1998;97(1):75–81.
- [37] Brown SB, Savill J. Phagocytosis triggers macrophage release of Fas ligand and induces apoptosis of bystander leukocytes. *J Immunol* 1999;162(1): 480–5.
- [38] Liles WC, Kiener PA, Ledbetter JA, Aruffo A, Klebanoff SJ. Differential expression of Fas (CD95) and Fas ligand on normal human phagocytes: implications for the regulation of apoptosis in neutrophils. *J Exp Med* 1996;184(2):429–40.
- [39] Richardson BC, Lalwani ND, Johnson KJ, Marks RM. Fas ligation triggers apoptosis in macrophages but not endothelial cells. *Eur J Immunol* 1994; 24(11):2640–5.